

# Graphene nanowalls for high-performance chemotherapeutic drug sensing and anti-fouling properties

Ioulia Tzouvadaki<sup>a,1</sup>, Nima Aliakbarinodehi<sup>a,\*,1</sup>, Diana Dávila Pineda<sup>b</sup>, Giovanni De Micheli<sup>a</sup>, Sandro Carrara<sup>a</sup>

<sup>a</sup> Integrated Systems Laboratory, École Polytechnique Fédérale de Lausanne, Lausanne, Switzerland

<sup>b</sup> IBM Research – Zurich, Rüschlikon, Switzerland

## ARTICLE INFO

### Article history:

Received 22 November 2017

Received in revised form 24 January 2018

Accepted 4 February 2018

Available online 6 February 2018

### Keywords:

Drug monitoring  
Graphene nanowalls  
Electrochemistry  
Etoposide  
Anti-fouling

## ABSTRACT

Improved sensitivity and continuous monitoring of therapeutic compounds are two of the most highlighted concerns for the treatment of malignant diseases, such as cancer. We demonstrated ultrasensitive screening of etoposide, a therapeutic compound widely-used in chemotherapy, achieved at low concentrations via the implementation of optimized graphene nanowalls.

The developed graphene nanowalls displayed excellent electrochemical sensing capabilities in the etoposide detection with regards to the drug therapeutic window, without any post-transfer procedures or any further surface treatment. The direct, catalyst-free, vertical growth of graphene nanostructures forming a honeycomb network on the substrate, was presented involving three different substrates and implementing different growth parameters. SEM, TEM and Raman spectroscopy techniques were implemented to verify the results.

The configuration that demonstrated the overall best performance in the sensing of electroactive compounds was selected and utilized for the effective screening of the drug resulting in a detection limit down to 4.36 nM. Moreover, the suggested sensors demonstrated excellent anti-fouling properties by removing in average the  $97.44 \pm 2.7\%$  of first etoposide peak and 100% of second peak after 3 cycles of cleaning in blank buffer; bringing solutions to a common problem of electroactive compound screening and highlighting the sensing capabilities for continuous monitoring of the drug.

© 2018 Elsevier B.V. All rights reserved.

## 1. Introduction

Cancer is a fatal malignant disease and a leading cause of death worldwide. Nevertheless, the systemic administration of anticancer drugs has laterally limited effectiveness in the treatment of solid tumors. In addition, the commonly applied therapeutic approaches signify invasive chemical treatments (chemotherapy) which are mainly toxic for the patient. As only a small fraction of the total dose of the drug reaches the tumor site, the remainder of the dose is distributed throughout healthy organs and tissues, causing undesirable side-effects. For dealing with this issue, the monitoring of the concentration of drug compounds in the

patient's circulating system is crucial for maintaining the drug concentrations within a targeted therapeutic window. This aims to the individualisation of the drug dosage regime for optimal efficacy and safety of the treatment, sparing expenses and side effects issues for the patients that the treatment would be harmful or inefficient. Furthermore, as opposed to traditional monitoring technologies, personalized therapy utilizing Point-of-Care (P.o.C) devices will provide a cutting-edge technology for economical and user-friendly monitoring of analytes directly available to patients. However, personalized therapy, presents some serious limitations and uncertainties while involving complexity when dealing with mass applications. Therefore, accurate techniques based on the quantitative monitoring of the drug response at any time after the administration is highly desirable.

Meanwhile, vertically-oriented graphene nanosheets (VGs) consisting of networks perpendicularly oriented to a substrate and demonstrating exposed sharp edges and pronounced surface-to-volume ratios, are recently reported in literature [1–4]. VGs can be grown on a wide variety of materials [1] completely or selectively filling the substrate, and may consist of only few-layers, i.e. 4–6

\* Corresponding author at: Integrated System Laboratory, École Polytechnique Fédérale de Lausanne, 1015, Lausanne, Switzerland.

E-mail addresses: [ioulia.tzouvadaki@epfl.ch](mailto:ioulia.tzouvadaki@epfl.ch) (I. Tzouvadaki), [nima.aliakbarinodehi@epfl.ch](mailto:nima.aliakbarinodehi@epfl.ch) (N. Aliakbarinodehi), [DDA@zurich.ibm.com](mailto:DDA@zurich.ibm.com) (D. Dávila Pineda), [giovanni.demicheli@epfl.ch](mailto:giovanni.demicheli@epfl.ch) (G. De Micheli), [sandro.carrara@epfl.ch](mailto:sandro.carrara@epfl.ch) (S. Carrara).

<sup>1</sup> These authors contributed equally.

atomic layers, of graphene [5] or being multi-layer graphene configurations forming wall-like networks known as graphene nanowalls (GNWs) [6]. GNWs have been leveraged in different applications, for example as enhancing materials for improving the interfacial strength of composites [7], or for ameliorating the electrochemical capabilities of electrodes, when the GNWs are coated on the electrode's surface [8]. In addition, applications involving GNWs in combination with other nanostructures, such as nanoparticles [9,10], or in conjugation with soft materials like Polydimethylsiloxane (PDMS) [11] are also reported for exhibiting improved performance. Nonetheless, very limited are the studies dedicated for implementation in the therapeutics field, and, most importantly, for the effective monitoring of chemotherapeutic drugs.

In this work, we demonstrated successful ultrasensitive detection of etoposide, one of the main drugs used in chemotherapy of cancer, achieving a Limit-of-Detection (LOD) down to 4.36 nM, by leveraging optimized graphene nanowalls developed by means of Thermal Chemical Vapor Deposition (TCVD) through a catalyst-free, direct-growth method. Graphene nanostructures were developed involving three different substrate materials and implementing different growth parameters with respect to growth time and gas flow ratios, and then compared for their sensing capabilities in monitoring electroactive compounds. The optimum configuration was then selected for the actual drug screening. The growth process was performed directly on the substrate that would shape the final electrochemical electrode, avoiding any complex transferring post-processes. The work targets at the crucial aspects of the therapeutics towards malignant diseases, such as improved sensitivity and detection within and below the concentrations of the therapeutic range. In addition, the aspect of the continuous drug monitoring is ensured by the excellent anti-fouling property exhibited by the graphene-based nanostructures.

## 2. Materials and methods

### 2.1. Growth process of vertically-stacked graphene network

A two-zone furnace thermal CVD (TCVD RF100CA 2D growth tool from Graphene Square Inc.) with a special tubular furnace design was used to implement the catalyst-free method for the growth of the nanostructures. For the preparation of samples, standard (100) 4" silicon wafers (Si-Mat) were employed as the starting substrate. A 300-nm oxide was grown using a thermal oxidation oven (Tempress TS6304) in the case of SiO<sub>2</sub> substrates. For the Ni substrates, a 20 nm Ni layer was directly deposited on Si substrates using an e-beam evaporator (Evatec BAK501 LL). Substrates were diced to single 1 cm × 2 cm chips, which were thoroughly cleaned in subsequent baths of acetone, IPA and water and dried prior the growth of the GNWs.

Subsequently, the chips were introduced horizontally inside the tube of the TCVD at room temperature. The chamber was first heated under a 20 sccm H<sub>2</sub> flow until reaching a temperature set point value of 750 °C, a generally preferable temperature condition for GNWs growth. Then, the temperature of the chamber was allowed to stabilize for 10 min under the same H<sub>2</sub> flow, followed by the catalyst-free, vertical growth of the two-dimensional graphene nanosheets. What followed was the catalyst-free, vertical growth of the two-dimensional graphene nano-sheets with honeycomb structure on the substrate. Methane (CH<sub>4</sub>) was used as the carbon source for the growth. The power for the RF plasma, the gas flow ratios, the growth time and the substrate material used are detailed in Fig. 1b. For all the runs, the pressure and temperature were monitored with constant reading values of 0.045 Torr and 750 °C respectively. The low pressure helped to achieve a more increased ionization rate and maintain the stability of the plasma. However, a

low pressure also meant a lower growth rate, while a higher plasma pressure allowed a larger volume of feedstock gas input, which could possibly realise the massive production of GNWs at a relatively high growth rate. After the growth of the nanostructures, the substrates were cooled under a 20 sccm H<sub>2</sub> flow till reaching room temperature and then removed from the chamber. No post-transfer was needed and the resulted graphene nanostructures were stored and ready for implementation in drug monitoring.

### 2.2. Evaluation of sensors performance and drug screening

For evaluating their performance in sensing electroactive species, the GNWs were implemented for the detection of ferrocyanide/ferricyanide solution. The electrochemical measurements were performed using an Autolab potentiostat/galvanostat workstation (PGSTAT128N) in 20 mL PBS (Phosphate-buffered saline 100 mM, pH 7.4 from Sigma) solution containing 10 mM ferrocyanide/ferricyanide redox couple. A three-electrode configuration, consisting of (a) the GNW-based electrode as WE, (b) a Platinum CE (MW-1032 Platinum wire auxiliary electrode (Pt) 7.5 cm from BASi) and (c) a RE (MF-2052 Electrode -RE-5B Ag/AgCl reference with flexible connector from BASi), protected in an electrode chamber (MF-2030 Double-junction reference electrode chamber from BASi), was implemented. All experiments were carried out in room temperature in PBS that was used as supporting electrolyte. The sensors were dipped in the solution under stirring conditions of 200 rpm to ensure a homogeneous solution.

The electrochemical response of electrodes was investigated by CV performed by sweeping the potential within the range from -800 mV to +1000 mV, with a scan rate of 110 mV/s. The different platforms with GNW-structures resulted from different growth parameters and substrates (same active electrode area of 1 × 1 cm of the WE dipped in the analyte solution) were characterized for their performance in the detection of ferrocyanide/ferricyanide, while the recorded characteristic oxidation peaks were considered as a first criterion of choosing the optimum GNW. These oxidation peaks were analysed with Nova software to obtain the peak amplitudes by removing the capacitive current from main Faradaic signal. The stability of the sensors was studied by obtaining cyclic voltammograms after successive washing step alternating with measurements in PBS (blank) and analyte detection. For this purpose, sensors based on GNWs electrodes fabricated on Ni, Si and SiO<sub>2</sub> substrates (refer to *Evaluation of GNWs in sensing of electroactive compounds*), were incubated in 20 mL 100 mM PBS solution and electrochemical measurements were implemented as mentioned above. The PBS baseline was obtained and after successive washing step alternating with measurements in PBS (blank) and analyte detection. For this purpose, sensors based on GNWs electrodes fabricated on Ni, Si and SiO<sub>2</sub> substrates (refer to *Evaluation of GNWs in sensing of electroactive compounds*), were incubated in 20 mL 100 mM PBS solution and electrochemical measurements were implemented as mentioned above. The PBS baseline was obtained and thereafter, measurements were performed via incubation in the solution and the peaks were clearly distinguished. The sensors were washed with MilliQ water and measurements in PBS were repeated for another two times to monitor the stability.

Etoposide powder purchased from Sigma-Aldrich (MW = 588.56 g/Mole) was first dissolved in 10 mMole/L methanol CH<sub>3</sub>OH (Sigma-Aldrich) to achieve a 2 mL of drug solution of 100 μM concentration (stock-solution). Then, the resulting etoposide solution was further diluted in 10 mM PBS (Sigma-Aldrich) to achieve the desired concentrations used in the following experiments. The direct interaction of etoposide with GNW-based biosensor was investigated through electrochemical measurements carried out using Autolab potentiostat/galvanostat (PGSTAT128N) and the optimum GNW-based electrodes as sensing

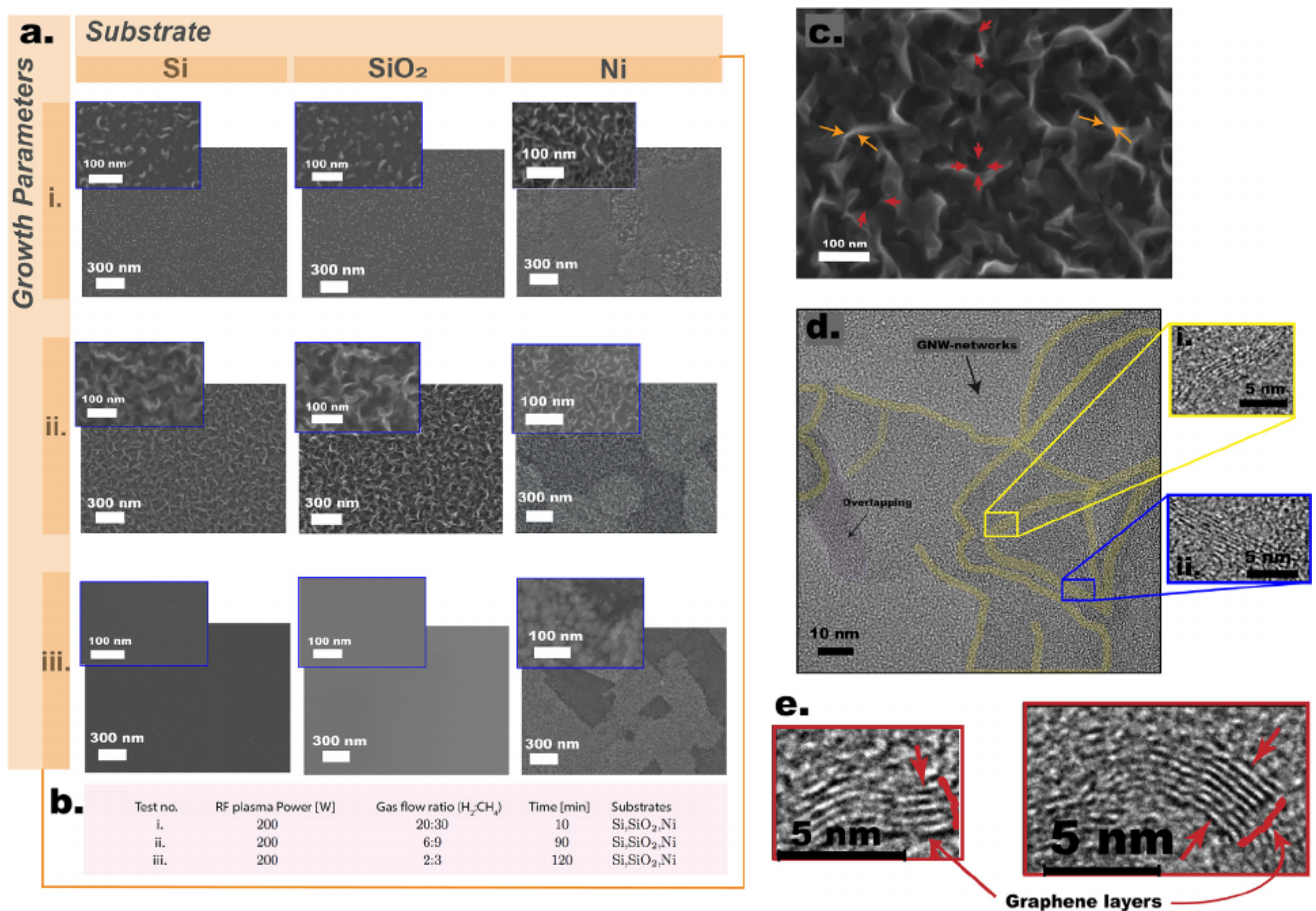


**Fig. 1.** SEM micrographs depicting the surface morphology of the GNW structures (a) acquired according to different growth parameters (b). The resulting nanostructures consist of sharp edges forming wall networks (orange arrows) of few nm, and cavity-like domains (red arrows) of some tens of nm that are formed between the neighbouring nanowalls (c). TEM characterization of the nanostructures reveals the GNW-network configurations (d) and the graphene layers that form the nanowall sidewalls (e). (For interpretation of the references to colour in this figure legend, the reader is referred to the web version of this article.)

elements and the optimum scan rate. Each electrode was first immersed in 20 mL of PBS, while Autolab was configured to sweep the voltage in the range of  $-0.4$  V to  $+0.8$  V using the scan rate of 110 mV. After the acquisition of the baseline in the blank buffer (0 M of etoposide), consecutive increasing drug concentration was introduced continuously in the buffer, starting from 50 nM of etoposide until 1  $\mu$ M, under continuous stirring conditions. A more intense stirring (500 rpm) was used each time that a new concentration of drug was introduced for enhancing the homogenisation of the solution and then the stirring was reset and kept constant at 200 rpm during the measurement procedure.

For drug screening using SWV again the same Autolab potentiostat/galvanostat was used to perform the measurements under aerobic conditions. To acquire the voltammograms, electrodes were immersed in PBS as mentioned above for CV, and voltage was swept between  $-0.4$  V and  $+1$  V. The step potential, stair amplitude and frequency of SWV was set to 5 mV, 20 mV and 10 Hz, respectively.

### 2.3. SEM and TEM analysis

SEM morphological characterization was performed for the GNWs fabricated with the various growth conditions and substrates. Scanning electron microscope Merlin from Zeiss working at 1.2–3 kV was used. TEM characterization was also performed using the transmission electron microscope from FEI (Talos F200X TEM) at high-resolution mode at 200 kV.

## 3. Results and discussion

### 3.1. GNWs morphological characterization

SEM characterization (bird-eye view of the surface morphology in lower and higher magnification imaging conditions) of the fabricated nanostructures (Fig. 1a) for the different growth parameters under consideration (Fig. 1b) reveals a “maze-like” configuration indicating the characteristic morphology and dimensions of GNWs. A further significant characteristic is the wavy geometry and the curled edges of the nanowalls that may be attributed to internal stress or/and to stress induced during the growth process. The nanostructures are aligned vertically to the substrate forming the typical honeycomb networks. More specifically, the resulted GNW-network is composed of domains covered with nanodomains and cavities depicting elliptical or cyclical shapes (Fig. 1c). These cavities are of approximately  $39.83 \pm 4.22$  nm for Si and of  $39.33 \pm 15.71$  nm for SiO<sub>2</sub>. The nanostructures obtained on a Ni substrate also demonstrate cavities, but slightly smaller of approximately  $23 \pm 6$  nm. Further, patterns are formed in the case of Ni substrate due to partial silicidation occurring as a result of the high process temperature (see Supplementary information).

The gas proportion and the growth time (Fig. 1b) play a significant role in the GNWs synthesis, influencing the nanostructures morphology [12]. However, it is usually hard to define a certain optimum gas ratio for all the different CVD systems. Many different examples are reported in literature for the acquisition of nanos-

structures by the implementation of different gas ratios and applied growth times. [6,7,11,13–16]

In the present work, it was found that a relatively short growth time (10 min) resulted in rough, incomplete structures indicating thicker sidewalls for both Si and SiO<sub>2</sub> ( $4.92 \pm 0.45$  nm and  $5.21 \pm 0.15$  nm respectively) due to the incomplete vertical growth of the nanomaterial despite the fact that a high gas flow ratio (H<sub>2</sub>:CH<sub>4</sub> at 20:30) was used. In the case of Ni substrate, no significant difference was generally observed that might be explained by the improved properties of the substrate that lead to a faster process. It is also worth to highlight that relatively low flow ratio (H<sub>2</sub>:CH<sub>4</sub> at 2:3), even combined with high growth time (120 min), barely yielded any nanostructure growth, and only the substrate was observed in the SEM morphological analysis (Fig. 1a.iii). This finding was further demonstrated by Raman spectroscopy (see Supplementary information). Nevertheless, the choice of an intermediate growth time (90 min) and a moderate flow ratio (6:9) resulted in successful growth of graphene nanowall structures (Fig. 1c.ii) demonstrating values of average sidewall thickness  $4.02 \pm 0.27$  nm,  $4.36 \pm 0.18$  nm and  $3.03 \pm 0.11$  nm for SiO<sub>2</sub>, Si and Ni substrates, respectively, avoiding saturation issues and time-consuming processes.

A very important aspect to take into account when fabricating GNW-structures is the layers of graphene that actually form the sidewalls of the final nanowall. Accumulated data acquired from SEM characterization, which encompassed several determinations regarding the sidewall of the GNWs and several measurements on different GNWs at multiple locations in all the fabricated samples, depicted an average thickness of the sidewalls of  $3.79 \pm 0.18$  nm that was in agreement with the values mentioned in literature. [1–4] Taking into account the interlayer spacing, that was reported with values of 0.34–0.37 nm and graphene monolayer thickness of 0.335–0.345 nm, it can be concluded that the produced nanowalls consist of an average of 5–7 graphene layers. This result agrees indeed with the Raman analysis, and the analysis of the full-width-half-maximum (FWHM) of the 2D peak (see Supplementary information).

In order to further analyse the aspect of the acquired nanowall thicknesses and the number of graphene sheets that actually shape the sidewalls of the nanostructures, TEM analysis was performed for the nanostructures resulted for SiO<sub>2</sub> substrate and the optimum growth parameters. TEM characterization (Fig. 1d) revealed stacking graphene sheets that form a self-supported network of wall structures with thicknesses in the range of few nm. The resulting GNW networks were demonstrated (and highlighted with colour). The edges of the suspended film always folded back allowing a cross-sectional view and making the changes in film thickness observable. Further TEM analysis (Fig. 1e), indicated sections of only few layers of graphene and confirmed the existence of interlayer spacing between the neighbouring graphene layers, a finding that is in good agreement with the SEM data. Overall, this topography scheme shaped the sidewalls of the GNW configurations.

### 3.2. Evaluation of GNWs in sensing of electroactive compounds

The obtained GNW electrodes were first characterized electrochemically for their performance in sensing of electroactive compounds through cyclic voltammetry (CV) using ferrocyanide/ferricyanide redox couple, a simple, yet widely known and used electroactive compound. A comparative analytical performance of the different GNW electrodes, acquired through the different growth parameters and substrate materials, was performed for the evaluation of their sensing capabilities (Fig. 2a). The GNWs acquired by implementing a growth time of 90 min and a flow ratio of 6:9, indicated the overall highest signal with respect to the peak-current and indicated more symmetric peaks

(CV peaks) (Fig. 2a -test ii-). On the contrary, low gas flow ratio of (2:3) and short growth times (10 min) resulted in incomplete growth of GNWs (Fig. 2a -test i and iii). This fact further validated the SEM (Fig. 1a) conclusions as well as the Raman spectroscopy findings (shown in the Supplementary information). A characteristic example was the case of growth on semi-conductive (Si) and on insulating (SiO<sub>2</sub>) substrates for low gas ratios -test iii-, where the outcomes were equivalent to those originated by plain substrates.

The sensing reproducibility after different successive and alternative steps in target and buffer solutions is another highly important aspect in electrochemistry. The electrochemical measurements presented in this work were repeated three times alternating buffer/target solutions, further validating the performance of the GNW sensors. More specifically, the expected peaks were indicated for same voltage values in good approximation (Fig. 2b), demonstrating notable reproducibility properties, along with high sensitivity and discrimination between the different compounds (PBS and ferrocyanide/ferricyanide) applied.

Taking into consideration the peak intensity and the stability, i.e. the reproducibility of the sensing output, of the sensors, voltammograms corresponding to nanostructures grown on Ni substrate, indicated higher CV peaks, but nevertheless with some slight offsets at their position. On the contrary, GNWs on SiO<sub>2</sub> substrate resulted to high CV peaks in combination with the advantage that the voltammograms were well overlapped, with insignificant differences in current amplitude (Fig. 2b). Therefore, the electrodes fabricated on SiO<sub>2</sub> substrate finally combined both high current peaks and good reproducibility qualities. As a conclusion, the GNWs electrodes fabricated on SiO<sub>2</sub> substrate using growth time of 90 min and a H<sub>2</sub>:CH<sub>4</sub> gas flow ratio of 6:9, result in an optimum performance in sensing electroactive compounds.

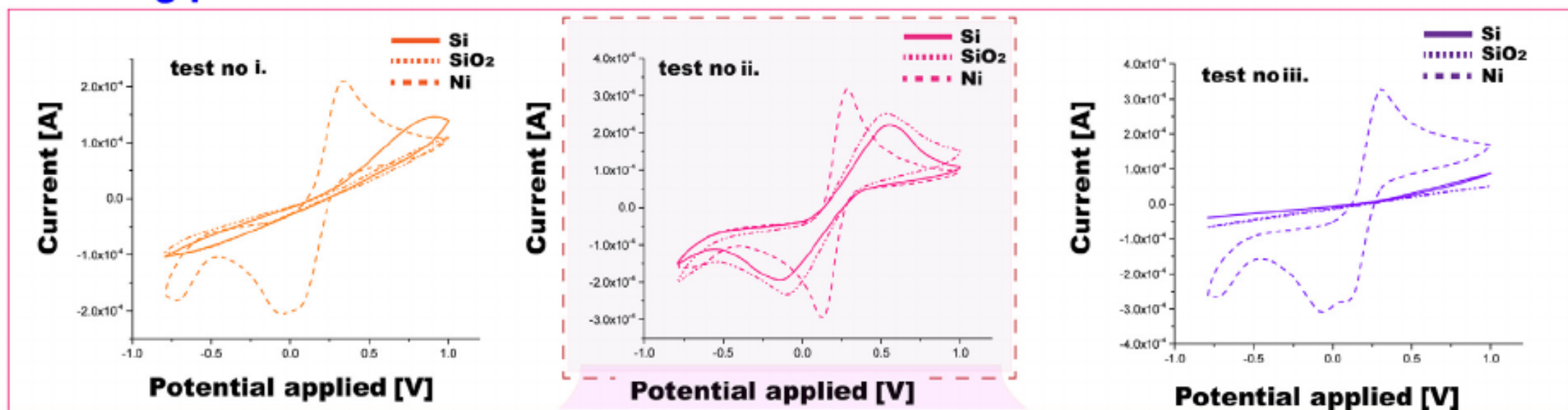
SEM morphological analysis of the surface of this sensor was carried out after the fabrication of the nanostructures before any electrochemical measurements, and after the completion of repeated measurements in ferrocyanide/ferricyanide electroactive compounds solution (Fig. 2c). Overall, the SEM micrographs acquired, were analysed for possible morphological defects, damages and surface modifications of the nanostructures due to the exposure to the analyte and the detection procedure. The surface of the nanostructures indicated significant stability after the repeated measurement procedure. The nanostructures well maintain their morphology, their initial form, and characteristics, based on SEM analysis that alongside the stable electrochemical response further validated the mechanical stability, and endurance of the GNW-based sensors.

### 3.3. Etoposide detection and anti-fouling properties

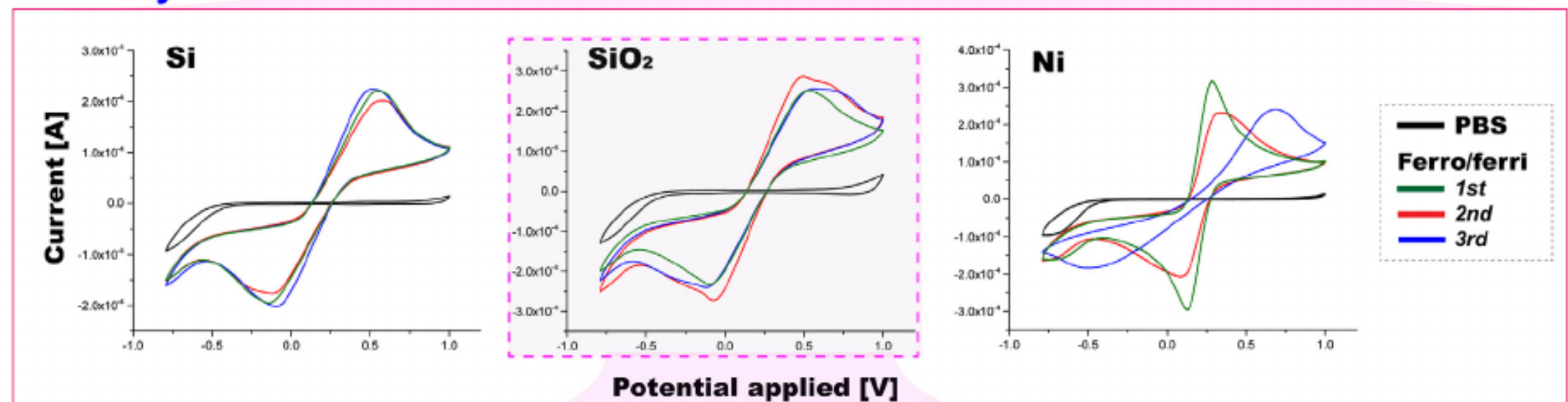
Etoposide is a drug widely-used in chemotherapy of various solid tumors. The effective therapeutic range for the etoposide has been reported from some tens of  $\mu\text{M}$  to  $100 \mu\text{M}$ . [17,18] For the etoposide detection, we have selected the GNW-based electrode that demonstrated remarkable performance both in terms of peak-height and stability, i.e. GNWs grown on a SiO<sub>2</sub> substrate following the growth conditions of test ii.

The electrochemical detection was first optimised by the investigation of the scan rate aspect (see Supplementary information). Then measurements were carried out using two electrochemical analysis techniques: CV and square wave voltammetry (SWV), this last one as a complementary technique, for increasing etoposide concentrations efficiently and detecting the drug below and within the drug therapeutic window. The obtained sensing results are shown in Fig. 3a for CV and in Fig. 3c for SWV. The peak amplitudes of three independent GNW-based electrodes were averaged and are presented here in Figs. 3b (for CV) and 3.d (for SWV). The obtained calibration curves, which are demonstrating the dose-

## a. Sensing performance



## b. Stability



## c.

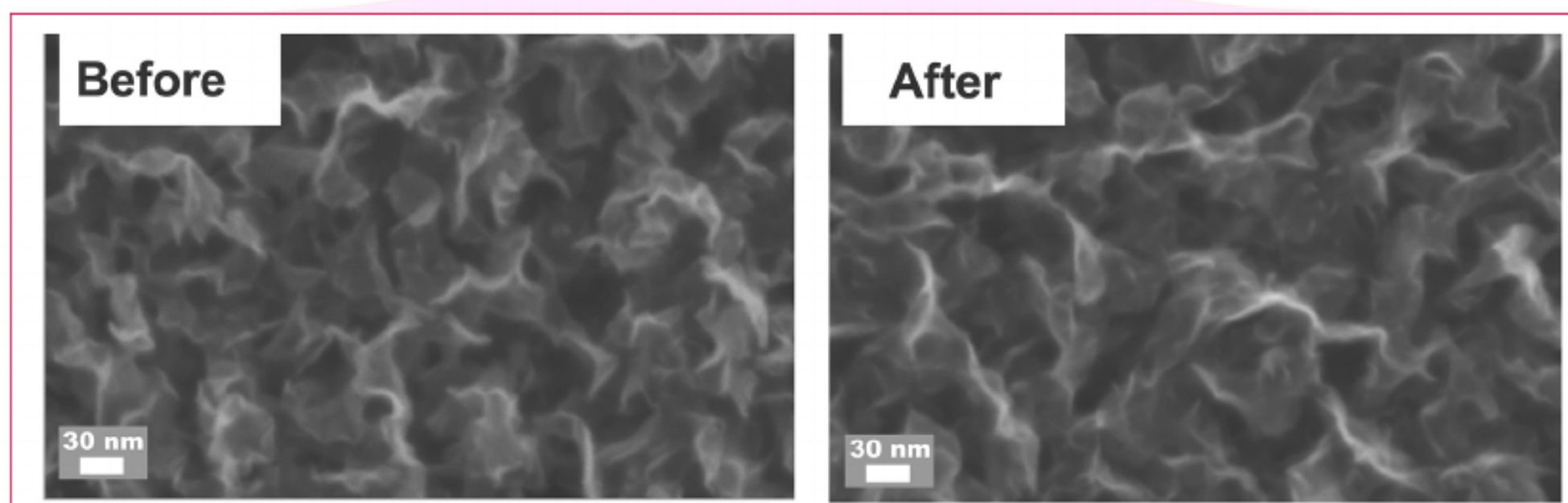


**Fig. 2.** Electrochemical characterization of the graphene-based electrodes of different substrate material and growth parameters for demonstrating the sensing performance (a) and the stability (b) of the electrodes in sensing electroactive compounds. SEM micrographs before and after the electrochemical measurements confirm that no defects, neither corrosion nor fouling occur at the morphology of the nanostructures (c).

response behaviour of biosensor for the specific target, follow a typical linear fitting equation for the case of CV and a third order equation for the case of SWV. The blank response was computed from the baseline noise for the average value and the standard deviation of blank for each case.

A LOD of 4.36 nM for CV and 24.7 nM for SWV have been calculated based on dose-response data using the method of Armbruster [19] utilizing three independent samples (see Supplementary information). It is worth to note that in general SWV is known to indicate better sensitivity, and in our case we have as well demonstrated higher discrimination and sensitivity with SWV comparing to CV. For instance, as presented in Fig. 3, for 200 nM of etoposide a signal of  $0.254 \pm 0.038 \mu\text{A}$  for CV and a signal of  $2.38 \pm 0.259 \mu\text{A}$  for SWV that is one order of magnitude higher in case of SWV. Nevertheless, the higher standard deviation measured in SWV consequently resulted in higher LOD compared to CV. The biosensor linear range for CV is of 0.05–1  $\mu\text{M}$  and 0.05–0.5  $\mu\text{M}$  for SWV. The hereby demonstrated LOD of 4.36 nM was compared to the state-of-the-art (Table 1) for different electrode configurations reported using voltammetric detection, and is highlighted as the best, to

**Table 1**

State-of-the-art list of electroactive drug detection to date for different electrode configurations reported using voltammetry, for etoposide detection.

Surface	LOD [nM]	Linear Range	Reference
CPE	100●●●	0.02–2.00 $\mu\text{M}$	[26]
GCE	17●●	0.06–100 $\mu\text{M}$	[27]
MWCNTs/GCE	5.4●●	0.02–2 $\mu\text{M}$	[24]
GNWs	4.36●	0.05–1/0.05–0.5 M	Present work

CPE: Carbon Paste Electrode, GCE: Glassy Carbon Electrode, MWCNTs: Multi-Walled Carbon Nanotubes.

●Buffer, ●●Britton-Robinson (BR) buffer, ●●●Serum.

our knowledge, so far reported LOD in the literature for an etoposide drug. This enhanced electrochemical performance of biosensor might be also attributed to the large surface area and good electrical conductivity of the graphene-based nanostructures. Moreover, the LOD obtained in this work suggests better performance comparing with other nanostructured biosensors for other well-known electroactive drugs (Propofol [20] and Theophylline [21]) as well as for electroactive metabolite correlated with drugs such as Dopamine

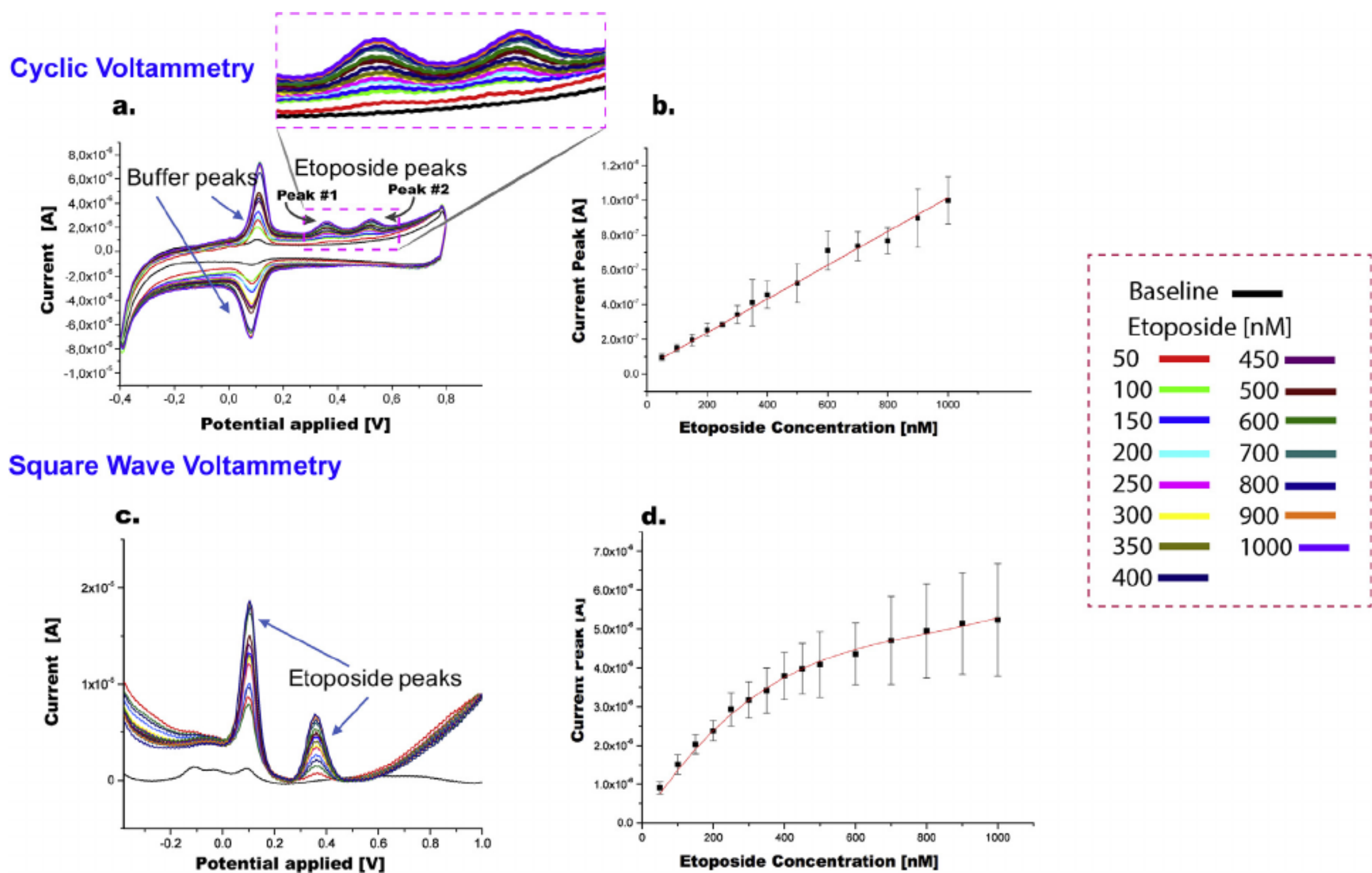


**Fig. 3.** Electrochemical characterization and the resulted peaks for CV (the characteristic peak of the PBS buffer and the two peaks of the drug noted as peak 1 and 2) (a) and the two peaks of the drug in (d) for SWV. The average peak amplitude for increasing etoposide concentrations is also shown for the two measurement methodologies applied (b,d).

[8,22,23], even though it should be noted that a direct comparison of the LOD for etoposide is not necessarily possible. As Table 1 presents, our platform reported similar ranges of sensitivity as the work with MWCNTs/GCE platform [24]. However, in the case of CNTs there are bio-fouling limitations that can be attributed to the large hydrophobic surfaces formed in the case of CNTs, as mentioned in the literature [24,25].

The performance of GNW-based electrodes was investigated for fouling side-effect phenomena, which can be attributed to the reaction products adsorbing on the sensing surface and forming electroactive films. Electrode fouling by electroactive compounds, as etoposide or propofol on carbon-based surfaces, is a widely reported phenomenon [24,25,28] that occurs due to adsorption of the analyte on the surface causing false responses even at blank solutions. This suppresses the electrochemical sensitivity and selectivity capabilities [22,23,25], and especially the potential use of electrodes in continuous monitoring, since electrodes have to be changed after each detection or go under complex cleaning procedures. Therefore, following the complete experimental procedure that finished with the detection of the highest drug concentration, the GNW-based electrodes were further studied regarding the aspect of fouling. To this aim, following the whole detection cycle experiments the electrodes were washed with DI water, and re-measured in blank buffer, a procedure that was repeated several times. The recorded results are presented in Fig. 4. It was observed in three experiments carried out on three different electrodes that the recorded drug-peak was significantly reduced after the first cycle and removed in-average by  $97.44 \pm 2.7\%$  for the first peak and 100% for second peak after the third cycle of measurements, indicating excellent anti-fouling properties of the presented GNW-based electrodes. This is a clear proof that the drug does not remain attached to the surface of the electrode after the electron exchange.

GNWs, as we demonstrated by Raman spectroscopy (Supplementary information), present a high D peak in the Raman spectra that according to the literature [29–31] is linked with high density of edge-plane like defects and consequently large density of functional groups such as carboxyl, epoxy, and hydroxyl improving hydrophilicity. This property ensures high water permeation and suppression of bio-fouling thanks to the low interfacial energy between a surface and water [32]. In addition, the negative charge of functional groups on the surface decrease the bio-fouling process of attachment of electroactive compounds on the electrode surface and their accumulation due to electrostatic repulsion characteristics [29]. Furthermore, an other general cause of bio-fouling is low kinetic of reaction at the surface that leads to the accumulation of the compound on the surface [33]. Thus, by increasing the electron transport and the kinetics, the bio-fouling can be suppressed. It is already reported in literature that graphene oxide surfaces have considerable density of reactive sites at sides and edge-plane-like defective sites, which leads to more kinetics of reaction and more efficient electrochemical performance [29,33]. Anti-fouling properties is a very alluring quality for an electrochemical sensor that allows re-usability, while ensuring stable sensitivity properties, thus, paving the way for continuous drug monitoring applications.

#### 4. Conclusions

The present work presents a first and innovative step towards the efficient detection of etoposide that is one of the widely used drugs in cancer chemotherapy that will also pave the way for further studies concerning interference and multiplexing aspects. The detection of etoposide is for the first time hereby reported by means of directly-grown GNW-structures. Different GNW configurations were developed implementing different sub-

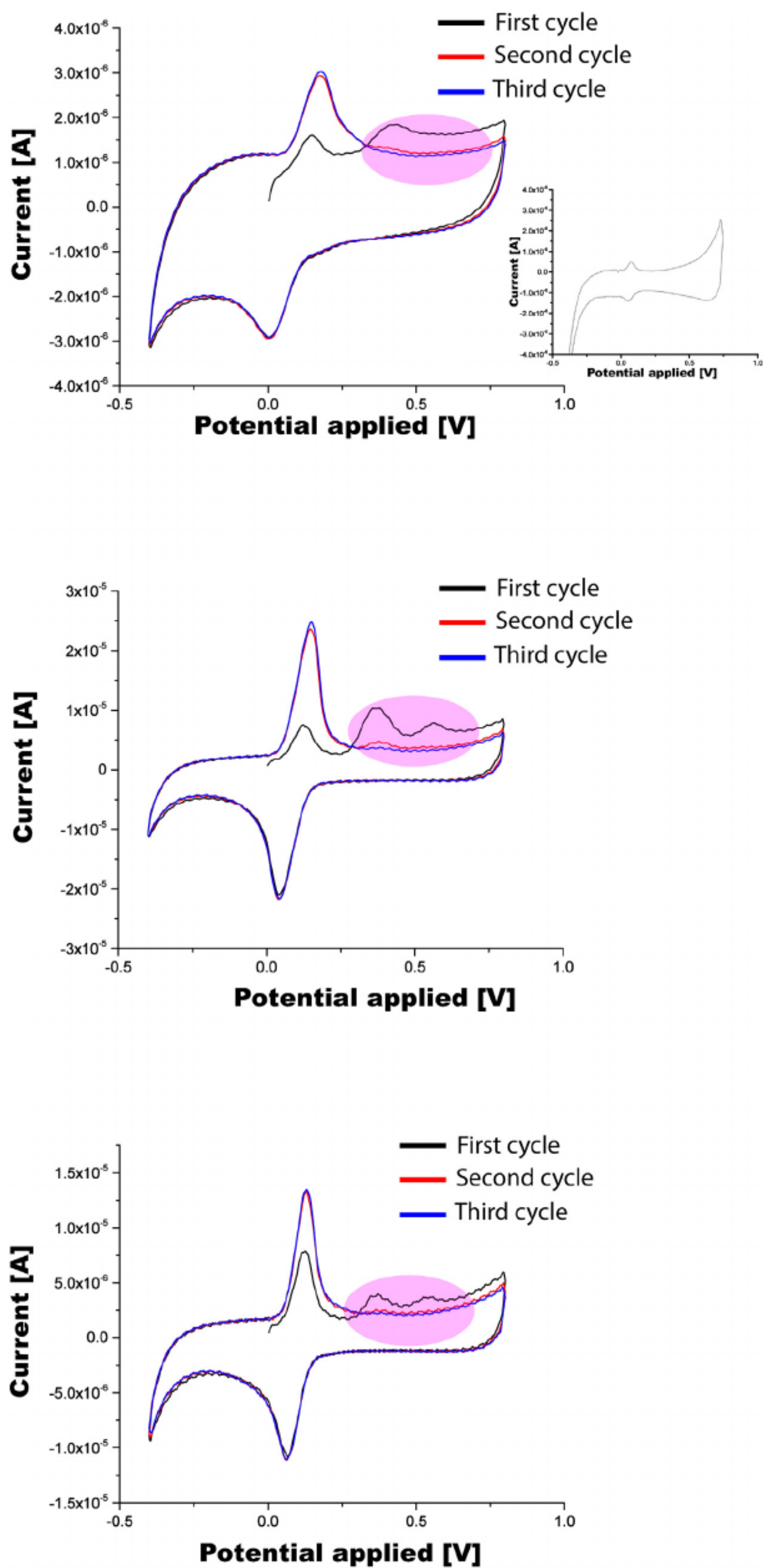


**Fig. 4.** Electrochemical characterization of three independent GNW-based electrodes indicating excellent anti-fouling properties. The recorded peaks of the drug, acquired during the performance of till three repeating cycles, removed in-average by  $97.44 \pm 2.7\%$  for the first peak and 100% for second peak after the third cycle of measurements.

strate materials and growth parameters and studied through SEM, TEM and Raman spectroscopy methods. The resulted nanostructures were first evaluated for their sensing capabilities through electrochemical characterization for successful detection of ferrocyanide/ferricyanide redox couple. Relatively low gas flow ratios and growth time resulted in incomplete growth of GNWs, with outcomes equivalent to those obtained by measurements using plain Si and SiO<sub>2</sub> substrates. While, the GNWs electrodes fabricated on SiO<sub>2</sub> substrate using growth time of 90 min and a flow rate of H<sub>2</sub>:CH<sub>4</sub> equal to 6:9 resulted in an optimum performance in terms of electrochemical biosensing and stability. These GNWs-based electrodes indicating optimum performance were applied for effective and successful screening of the chemotherapeutic drug below and within the therapeutic window, using CV and SWV with optimised scan rate for increasing the detection performance.

Overall, the GNWs display excellent performance for drug screening at concentration below and within the lowest values of the therapeutic window paving the way for the estimation of the drug's effectiveness, and results to a LOD of 4.36 nM in electrochemical response towards the etoposide detection. Moreover, the GNWs-platform exhibits significant anti-fouling properties, a fact that is demonstrated by measurement cycles in blank after completing the full drug-sensing procedure that removed in-average the drug peaks by 97.44 ± 2.7% for the first peak, and 100% for second peak after the third cycle of measurements. Moreover, the suggested nanostructure-based electrodes do not require any post-transferring procedures or any further surface treatment for achieving optimum performance, and can be directly implemented for highly sensitive drug sensing.

#### Author contributions

T and N.A contributed equally. I.T and N.A performed all surface treatments, data acquisition, data analysis, SEM and TEM imaging and comparison with the literature. I.T, D.D and N.A performed fabrications and Raman analysis. I.T and N.A have prepared the manuscript. S.C and D.D gave suggestions on the manuscript. I.T, N.A, D.D, S.C, and G.d.M have revised the manuscript.

#### Acknowledgements

The authors thank D. Deiana for assisting with TEM characterization. The authors acknowledge financial support from European Commission FP7 Programme through the Marie Curie Initial Training Network 'PROSENSE' (Grant No. 317420, 2012–2016), and by H2020-ERC-2014-ADG669354 CyberCare.

#### Appendix A. Supplementary data

Supplementary data associated with this article can be found, in the online version, at <https://doi.org/10.1016/j.snb.2018.02.036>.

#### References

- [1] K. Davami, Y. Jiang, J. Cortes, C. Lin, M. Shaygan, K.T. Turner, I. Bargatin, Tuning the mechanical properties of vertical graphene sheets through atomic layer deposition, *Nanotechnology* 27 (2016) 155701.
- [2] W. Li, Z. Zhang, Y. Tang, H. Bian, T.-W. Ng, W. Zhang, C.-S. Lee, Graphene-nanowall-decorated carbon felt with excellent electrochemical activity toward VO<sub>2</sub><sup>+</sup>/VO<sub>2</sub> couple for all vanadium redox flow battery, *Adv. Sci.* 3 (2016) <http://onlinelibrary.wiley.com/doi/10.1002/adv.201500276/full>.
- [3] K. Yu, P. Wang, G. Lu, K.-H. Chen, Z. Bo, J. Chen, Patterning vertically oriented graphene sheets for nanodevice applications, *J. Phys. Chem. Lett.* 2 (2011) 537–542.
- [4] J. Fang, I. Levchenko, S. Kumar, D. Seo, K.K. Ostrikov, Vertically-aligned graphene flakes on nanoporous templates: morphology, thickness, and defect level control by pre-treatment, *Sci. Technol. Adv. Mater.* 15 (2014) 55009.
- [5] A. Malesevic, R. Vitchev, K. Schouteden, A. Volodin, L. Zhang, G. Van Tendeloo, A. Vanhulsel, C. Van Haesendonck, Synthesis of few-layer graphene via microwave plasma-enhanced chemical vapour deposition, *Nanotechnology* 19 (2008) 305604.
- [6] Y. Wu, B. Yang, B. Zong, H. Sun, Z. Shen, Y. Feng, Carbon nanowalls and related materials, *J. Mater. Chem.* 14 (2004) 469–477.
- [7] Y. Chi, J. Chu, M. Chen, C. Li, W. Mao, M. Piao, H. Zhang, B.S. Liu, H. Shi, Directly deposited graphene nanowalls on carbon fiber for improving the interface strength in composites, *Appl. Phys. Lett.* 108 (2016) 211601, <http://dx.doi.org/10.1063/1.4952593>.
- [8] F. Tian, H. Li, M. Li, C. Li, Y. Lei, B. Yang, A tantalum electrode coated with graphene nanowalls for simultaneous voltammetric determination of dopamine, uric acid L-tyrosine, and hydrochlorothiazide, *Microchim. Acta* 184 (2017) 1611–1619.
- [9] S. Mao, K. Yu, J. Chang, D.A. Steeber, L.E. Ocola, J. Chen, Direct growth of vertically-oriented graphene for field-effect transistor biosensor, *Sci. Rep.* 3 (2013) <https://www.ncbi.nlm.nih.gov/pmc/articles/PMC3631944/>.
- [10] K. Mase, H. Kondo, S. Kondo, M. Hori, M. Hiramatsu, H. Kano, Formation and mechanism of ultrahigh density platinum nanoparticles on vertically grown graphene sheets by metal-organic chemical supercritical fluid deposition, *Appl. Phys. Lett.* 98 (2011) 193108, <http://dx.doi.org/10.1063/1.3583672>.
- [11] J. Yang, D. Wei, L. Tang, X. Song, W. Luo, J. Chu, T. Gao, H. Shi, C. Du, Wearable temperature sensor based on graphene nanowalls, *RSC Adv.* 5 (2015) 25609–25615.
- [12] M. Li, D. Liu, D. Wei, X. Song, D. Wei, A.T.S. Wee, Controllable synthesis of graphene by plasma-enhanced chemical vapor deposition and its related applications, *Adv. Sci.* 3 (2016) <http://onlinelibrary.wiley.com/doi/10.1002/adv.201600003/full>.
- [13] Y. Kim, W. Song, S.Y. Lee, C. Jeon, W. Jung, M. Kim, C.-Y. Park, Low-temperature synthesis of graphene on nickel foil by microwave plasma chemical vapor deposition, *Appl. Phys. Lett.* 98 (2011) 263106.
- [14] J. Wang, M. Zhu, R.A. Outlaw, X. Zhao, D.M. Manos, B.C. Holloway, Synthesis of carbon nanosheets by inductively coupled radio-frequency plasma enhanced chemical vapor deposition, *Carbon* 42 (2004) 2867–2872.
- [15] Z. Bo, Y. Yang, J. Chen, K. Yu, J. Yan, K. Cen, Plasma-enhanced chemical vapor deposition synthesis of vertically oriented graphene nanosheets, *Nanoscale* 5 (2013) 5180–5204.
- [16] X. Song, J. Liu, L. Yu, J. Yang, L. Fang, H. Shi, C. Du, D. Wei, Direct versatile PECVD growth of graphene nanowalls on multiple substrates, *Mater. Lett.* 137 (2014) 25–28.
- [17] K.R. Hande, P.J. Wedlund, R.M. Noone, G.R. Wilkinson, F.A. Greco, S.N. Wolff, Pharmacokinetics of high-dose etoposide (VP-16-213) administered to cancer patients, *Cancer Res.* 44 (1984) 379–382.
- [18] S.G. Arbuck, H.O. Douglass, W.R. Crom, P. Goodwin, Y. Silk, C. Cooper, W.E. Evans, Etoposide pharmacokinetics in patients with normal and abnormal organ function, *J. Clin. Oncol.* 4 (1986) 1690–1695.
- [19] D.A. Armbruster, T. Pry, Limit of blank, limit of detection and limit of quantitation, *Clin. Biochem. Rev.* 29 (2008) S49–52.
- [20] F. Kivlehan, E. Chaum, E. Lindner, Propofol detection and quantification in human blood: the promise of feedback controlled closed-loop anesthesia, *Analyst* 140 (2015) 98–106.
- [21] S. MansouriMajd, H. Teymourian, A. Salimi, R. Hallaj, Fabrication of electrochemical theophylline sensor based on manganese oxide nanoparticles/ionic liquid/chitosan nanocomposite modified glassy carbon electrode, *Electrochim. Acta* 108 (2013) 707–716.
- [22] H. Dong, S. Wang, A. Liu, J.J. Galligan, G.M. Swain, Drug effects on the electrochemical detection of norepinephrine with carbon fiber and diamond microelectrodes, *J. Electroanal. Chem.* 632 (2009) 20–29.
- [23] C. Davidson, E.H. Ellinwood, S.B. Douglas, T.H. Lee, Effect of cocaine, nomifensine GBR 12909 and WIN 35428 on carbon fiber microelectrode sensitivity for voltammetric recording of dopamine, *J. Neurosci. Methods* 101 (2000) 75–83.
- [24] B. Bozal-Palabiyik, B. Dogan-Topal, B. Uslu, A. Can, S.A. Ozkan, Sensitive voltammetric assay of etoposide using modified glassy carbon electrode with a dispersion of multi-walled carbon nanotube, *J. Solid State Electrochem.* 17 (2013) 2815–2822, <http://dx.doi.org/10.1007/s10008-013-2184-2>.
- [25] N. Aliakbarinodehi, G. De Micheli, S. Carrara, Enzymatic and nonenzymatic electrochemical interaction of abiraterone (antiprostata cancer drug) with multiwalled carbon nanotube bioelectrodes, *Anal. Chem.* 88 (2016) 9347–9350, <http://dx.doi.org/10.1021/acs.analchem.6b02747>.
- [26] A.-E. Radi, N. Abd-Elghany, T. Wahdan, Electrochemical study of the antineoplastic agent etoposide at carbon paste electrode and its determination in spiked human serum by differential pulse voltammetry, *Chem. Pharm. Bull. (Tokyo)* 55 (2007) 1379–1382.
- [27] H.V. Nguyen, L. Richtera, A. Moullick, K. Xhaxhiu, J. Kudr, N. Cernei, H. Polanska, Z. Heger, M. Masarik, P. Kopel, et al., Electrochemical sensing of etoposide using carbon quantum dot modified glassy carbon electrode, *Analyst* 141 (2016) 2665–2675.
- [28] F. Stradolini, T. Elboshra, A. Biscotini, G. De Micheli, S. Carrara, Simultaneous monitoring of anesthetics and therapeutic compounds with a portable multichannel potentiostat, *Circuits Syst. ISCAS 2016 IEEE Int. Symp. On, IEEE* (2016) 834–837 <http://ieeexplore.ieee.org/abstract/document/7527370/>.
- [29] J. Lee, H.-R. Chae, Y.J. Won, K. Lee, C.-H. Lee, H.H. Lee, I.-C. Kim, J. Lee, Graphene oxide nanoplatelets composite membrane with hydrophilic and antifouling properties for wastewater treatment, *J. Membr. Sci.* 448 (2013) 223–230, <http://dx.doi.org/10.1016/j.memsci.2013.08.017>.
- [30] K. Davami, M. Shaygan, N. Kheirabi, J. Zhao, D.A. Kovalenko, M.H. Rummeli, J. Opitz, G. Cuniberti, J.-S. Lee, M. Meyyappan, Synthesis and characterization of

carbon nanowalls on different substrates by radio frequency plasma enhanced chemical vapor deposition, *Carbon* 72 (2014) 372–380.

- [31] F. Banhart, J. Kotakoski, A.V. Krasheninnikov, Structural defects in graphene, *ACS Nano* 5 (2010) 26–41.
- [32] S. Zinadini, A.A. Zinatizadeh, M. Rahimi, V. Vatanpour, H. Zangeneh, Preparation of a novel antifouling mixed matrix PES membrane by embedding graphene oxide nanoplates, *J. Membr. Sci.* 453 (2014) 292–301, <http://dx.doi.org/10.1016/j.memsci.2013.10.070>.
- [33] A. Noorbakhsh, A.I.K. Alnajjar, Antifouling properties of reduced graphene oxide nanosheets for highly sensitive determination of insulin, *Microchem. J.* 129 (2016) 310–317, <http://dx.doi.org/10.1016/j.microc.2016.06.009>.

## Biographies

**Ioulia Tzouvadaki** received her B.Sc. degree in physics, from National and Kapodistrian University of Athens (U.O.A), Greece, the M.Sc. degree in microsystems and nanodevices from National Technical University of Athens (N.T.U.A) and the doctorate degree from EPFL, Switzerland. During her postgraduate studies, she worked at the Clean Room Laboratory of the National Center for Scientific Research (NCSR) Demokritos in the field of experimental construction processes concerning integrated circuits and the experimental characterisation process of nanomaterials and nanodevices. Her M.Sc. thesis concerned the computational study and simulation of polymer nanocomposite materials, within the Computational Materials Science and Engineering (CoMSE) research group, of the School of Chemical Engineering at the NTUA. Her Ph.D. work at the Integrated System Laboratory (LSI) of EPFL, focused on the fabrication and characterisation of nanostructures and their implementation as ultrasensitive nano-bio-sensors in both diagnostics and therapeutics.

**Nima Aliakbarinodahi** has obtained his PhD from Integrated Systems Laboratory (LSI) at École Polytechnique Fédérale de Lausanne (EPFL), Switzerland. He is currently investigating the development of ultrasensitive electrochemical and field-effect biosensors for diseases theragnosis (diagnosis and therapy). Nima, born in Tehran on 1986, received his B.Sc. from Mazandaran University, Iran in Electronics. He continued his M.Sc. study in Politecnico di Torino, Italy in MEMS, where he achieved a scholarship from LSI for a 6 months master thesis exchange program at EPFL. During his master thesis he worked on the optimization of electrochemical biosensors with the aim of enhancing their sensing performance and reliability.

**Diana Dávila Pineda** is currently an Adv. Senior Engineer at the IBM Research – Zurich Lab. She received her B.Sc. in Electronic Engineering, from the Tecnológico de Monterrey, Mexico in 2004 and her M.S. in Micro and Nanoelectronic Engineering in 2008 and Ph.D. in Electronic Engineering in 2011 from the Universitat Autònoma de Barcelona, Spain. She has conducted research on fuel cells, nanomaterials, thermoelectricity, spintronics and MEMS devices in multidisciplinary environments such as the Microelectronics Institute of Barcelona (IMB-CNM, CSIC), the Catalonia Institute for Energy Research (IREC), the International Iberian Nanotechnology Laboratory (INL) and ETH Zurich.

**Giovanni De Micheli** is Professor and Director of the Institute of Electrical Engineering and of the Integrated Systems Centre at EPF Lausanne, Switzerland. He is program leader of the Nano-Tera.ch program. Previously, he was Professor of Electrical Engineering at Stanford University. He holds a Nuclear Engineer degree (Politecnico di Milano, 1979), a M.S. and a Ph.D. degree in Electrical Engineering and Computer Science (University of California at Berkeley, 1980 and 1983). Prof. De Micheli is a Fellow of ACM and IEEE, a member of the Academia Europaea and an International Honorary member of the American Academy of Arts and Sciences. His research interests include several aspects of design technologies for integrated circuits and systems, such as synthesis for emerging technologies, networks on chips and 3D integration. He is also interested in heterogeneous platform design including electrical components and biosensors, as well as in data processing of biomedical information. He is author of: *Synthesis and Optimization of Digital Circuits*, McGraw-Hill, 1994, co-author and/or co-editor of eight other books and of over 750 technical articles. His citation h-index is 93 according to Google Scholar. He is member of the Scientific Advisory Board of IMEC (Leuven, B), CFAED (Dresden, D) and STMicroelectronics.

**Sandro Carrara** is an IEEE Fellow for his outstanding record of accomplishments in the field of design of nanoscale biological CMOS sensors. He is also the recipient of the IEEE Sensors Council Technical Achievement Award in 2016 for his leadership in the emerging area of co-design in Bio/Nano/CMOS interfaces. He is a faculty member (MER) at the EPFL in Lausanne (Switzerland). He is former professor of optical and electrical biosensors at the Department of Electrical Engineering and Biophysics (DIBE) of the University of Genoa (Italy) and former professor of nanobiotechnology at the University of Bologna (Italy). He holds a PhD in Biochemistry & Biophysics from University of Padua (Italy), a Master degree in Physics from University of Genoa (Italy), and a diploma in Electronics from National Institute of Technology in Albenga (Italy). His scientific interests are on electrical phenomena of nano-bio-structured films, and include CMOS design of biochips based on proteins and DNA.